ELSEVIER

Analytica Chimica Acta 466 (2002) 1–9

ANALYTICA CHIMICA ACTA

www.elsevier.com/locate/aca

Aerosol analysis by cavity-ring-down laser spectroscopy

Valery Bulatov*, Michal Fisher, Israel Schechter

Department of Chemistry, Technion-Israel Institute of Technology, Haifa 32000, Israel

Received 1 March 2002; received in revised form 5 June 2002; accepted 5 June 2002

Abstract

The cavity-ring-down technique was applied for aerosol detection. The experimental set-up was based on a pulsed dye laser pumped with the third harmonic of an Nd:YAG laser. Validation of the method was performed using calibrated aerosol flows, all under ambient conditions. The method was exemplified with non-absorbing aerosols, such as NaCl and $CuCl_2{\cdot}2H_2O$, of various sizes and concentrations. The results were used for the evaluation of the corresponding aerosol extinction coefficients as a function of size, shape and index of refraction. The thus obtained aerosol extinction efficiencies were compared to theoretical models. Good agreement with theory was observed for NaCl aerosols, while the results for $CuCl_2{\cdot}2H_2O$ particulates required averaging over particle size and over the orientation dependent index of refraction. The actual sensitivity currently achieved was as low as an extinction coefficient of 8×10^{-8} cm^{-1}, which means detection capability of about six water micro-particulates per cm^3. The ultimate theoretical performance of this method for aerosol detection was estimated as an extinction coefficient of 1.4×10^{-12} cm^{-1}, corresponding to about 100 micro-particulates per m^3. These figures indicate that this method has the potential to become one of the most sensitive on-line analytical technique for aerosol detection and quantification.

Keywords: Aerosol; CRLAS; Laser; Analysis; Ring-down; Particulates

1. Introduction

The basic principles of cavity-ring-down laser absorption spectroscopy (CRLAS), as developed by O'Keefe and Deacon [1], are very simple and the method has been widely reviewed [2–6]. In short, the light pulse produced by a tuneable laser is injected into an optical cavity formed by two highly reflecting mirrors. Under these conditions, the laser pulse, which is partially transmitted into the cavity by the input mirror, travels many (typically several thousands) round trips inside the cavity. The light intensity (partially transmission through the output mirror), decays due to losses in the system. This decay is characterized by the so-called cavity-ring-down time. If an absorbing or scattering sample is placed inside the cavity under the above conditions, the cavity-ring-down time is shortened at those specific wavelengths where absorption occurs.

The detector, placed after the exit mirror, encounters a sequence of pulses (essentially much less intense replicas of the original laser pulse) emerging from the cavity, temporally separated by the cavity round-trip time $2L/c$ (where L is a cavity length). A simple exponential decay envelope caused by the cavity losses is obtained. The intensity of these pulses as a function of time (t) is described by:

$$I = I_0 \exp\left(\frac{-t}{t_c}\right) \quad (1)$$

where t_c is the characteristic lifetime of laser pulse in the optical cavity.

* Corresponding author. Fax: +972-4829-2579.
E-mail address: israel@techunix.technion.ac.il (I. Schechter).

0003-2670/02/$ – see front matter
PII: S0003-2670(02)00516-0

If an absorbing (or scattering) sample is placed inside the cavity, we get:

$$\frac{1}{t_c} = \frac{\sigma c l}{nL} + \frac{1}{t_c^0} \quad (2)$$

or

$$\frac{1}{t_c} - \frac{1}{t_c^0} = \frac{\sigma c l}{nL} \quad (3)$$

where t_c^0 is the characteristic lifetime of a laser pulse in the optical cavity occupied with merely dry air, σ the sample extinction coefficient, l the length of the absorbing medium and n is the refraction index of the medium inside the cavity.

One of the most important advantages of CRLAS in analytical measurements is its high sensitivity. Recent advances allow for detection of absorbance as low as 10^{-9} [7,8] or even 10^{-10} [5,9,10] per cm of the optical path. Besides its potential for high sensitivity, CRLAS is a rather simple method that can readily be realized. Wavelength tuning in a wide spectral range (UV–IR) enables the detection of large variety of species.

A brief description of most relevant current **analytical applications** of CRLAS is hereby provided. We first refer to the recent gas phase applications.

One of the major benefits of CRLAS is its ability to provide structural information regarding transient molecules and clusters in molecular beams. Recent examples are applications to metal clusters and metal-containing molecules [11,12]. CRLAS in the IR range has been applied to the study of bending vibrations in water cluster $(H_2O)_n$. Intermolecular vibrations could be measured by this method, providing information on both structures and hydrogen bond rearrangement dynamics [13,14]. The capability of measuring absolute concentration of water clusters has been applied in atmospheric in situ studies. IR–CRLAS has also been used in studying the O–H stretching vibrations of jet-cooled alcohol clusters [15–17].

CRLAS is already a well-established method for analysis of trace gases and vapors. Ambient concentration of NO_2 was determined by CLRAS more than a decade ago, with detection limit below 1 ppb for the 0.5 m cavity used [18]. The detection limit for Hg, measured at ambient conditions, was ca. 0.50 ppt [19]. CRLAS has also been applied to sensitive atmospheric detection of nitrate radical [20] and to measurements of isotopic ratio of methane (detection limit of 105 ppt) [21]. These figures demonstrate the potential of CRLAS in air pollution monitoring.

CRLAS has also been applied in the study of transient species present in flames and plasmas. The advantage of CRLAS in this area is its ability of providing both spectral and spatial resolution. Several radicals were detected in a low-pressure methane/oxygen/nitrogen flames [22–25]. Kinetic studies related to flame radicals were also extensively investigated [26–30]. Besides concentration measurements, CRLAS was extended for the evaluation of losses in thin films, 2–20 μm thickness [31].

Only recently, a few studies related to airborne particulates have been published [32–34]. A non-resonant cavity-ring-down set-up for measuring light attenuation by atmospheric particulates at wavelength of 532 and 355 nm was described. The results were compared with those obtained by commercially available instruments [32].

The cavity-ring-down technique was also applied for measuring absorption losses due to carbonaceous and soot particles. The soot volume fraction was determined in flame [34]. A system for direct determination of the optical extinction of airborne particulates was suggested and it was suggested that such measurements may be useful for separating the scattering and absorption components of the measured extinction [33].

This paper suggests a new application of CRLAS to aerosol analysis, therefore, besides the analytical applications, we need to introduce some concepts on **optical properties of aerosols** [35,36]:

Aerosol particles, illuminated by a light beam, scatter and absorb some of that light, thereby diminish the intensity of the beam. This process is called *extinction* and addresses only the attenuation of light along the optical axis. The scattering in each case is governed by the ratio of the particle diameter, d, to the wavelength, λ, of the radiation. This dimensionless ratio is called the *size parameter*, α, and is given by:

$$\alpha = \frac{\pi d}{\lambda} \quad (4)$$

While all aerosol particles scatter light, only those composed of absorbing material will absorb. The ratio of the light intensity, I, traversing the aerosol, to that

incident on the aerosol, I_0, is described by:

$$I = I_0 \exp(-\sigma_e L) \quad (5)$$

where σ_e is the *aerosol extinction coefficient* (the subscript differentiates from the sample coefficient, due to the absorption and scattering) and L is the path length of the light beam through the aerosol. The aerosol extinction coefficient σ_e is given by:

$$\sigma_e = \varepsilon Q_e N \quad (6)$$

where ε is the cross-section of the aerosol particle, N the number concentration of the aerosol particles and Q_e is the *particle extinction efficiency*, defined as:

$$Q_e = \frac{\text{radiant power scattered and absorbed by a particle}}{\text{radiant power geometrically incident on the particle}} \quad (7)$$

Therefore, for mono-dispersed aerosol of N spherical particles per unit volume, the aerosol extinction coefficient is simply given by:

$$\sigma_e = \tfrac{1}{4}\pi N d^2 Q_e \quad (8)$$

The particle extinction efficiency times the projected area of a particle is the cross-sectional area of light removed from a beam by the particle. Q_e=2.0 indicates that a particle removes twice as much light as it would by simple projected-area blocking. Values of Q_e range from 0 to about 5 for spherical particles and to about 15–20 for prolate spheroids with main axis ratio of 4.0–5.0, e.g. [36].

The extinction efficiency of a particle is the sum of its scattering efficiency Q_S and its absorption efficiency Q_a,

$$Q_e = Q_S + Q_a \quad (9)$$

where Q_S and Q_a are defined by equations equivalent to Eq. (7). From Eq. (9) we obtain that, for mono-dispersed particles:

$$\sigma_e = \sigma_s + \sigma_a \quad (10)$$

where σ_s and σ_a are defined by Eq. (8) with Q_e being replaced by Q_S and Q_a, respectively. For non-absorbing particles, $Q_e = Q_S$ and $\sigma_e = \sigma_s$.

When poly-dispersed aerosols are concerned, Eq. (8) holds for each particle size and the combined effect is given by the sum of contributions of all the particle sizes. However, for mono-dispersed aerosols, σ_e can be calculated by Eq. (8), provided that Q_e values are known. The latter depend on the particle refractive index, shape and size relative to the wavelength of light. For **small particles**, d <0.05 μm, Q_e can be calculated directly from the next equation, following the Rayleigh scattering theory (e.g. [36]):

$$Q_e = \frac{8}{3}\left(\frac{\pi d}{\lambda}\right)^4 \left(\frac{n^2-1}{n^2+2}\right)^2 \quad (11)$$

where n is the particle refractive index. For **large particles** (d >4 μm), Q_e approaches its limiting value of 2.0, after some oscillations and for strongly absorbing particles it approached the same value without oscillations (e.g. [36]). For **medium particles** between 0.05 and 4 μm (the Mie scattering region), there is no simple equation for Q_e, and its value can be obtained using computer calculations [37–40]. In the general case, Q_e has to be calculated using the Bohren and Huffman algorithm [36].

2. Experimental

2.1. Optical system

The experimental arrangement is shown in Fig. 1. Two concave mirrors (VLOC Corporation, USA), curvature radii of 50 cm, formed the ring-down cavity. Both mirrors had specified reflectivity of about 99.95% with maximum at λ = 620 nm. The length of the ring-down cavity was 75 cm. A slow flow of dry clean nitrogen was introduced near the mirrors in order to protect them and minimize contamination by aerosols particles.

The laser source was the third harmonic generation of a Nd:YAG laser (Continuum, Powerlite-8010, USA). It pumped a dye laser (PTI Corporation, USA, 0.5 cm^{-1} resolution, 100 μJ). The laser scanning region was between 595 and 645 nm, and most measurements were carried out at λ = 620 nm.

The output of the dye laser was focused and spatially filtered by means of 1:2 telescope, equipped with 100 μm pinhole aperture. The beam diameter was 2 mm before coupling into the optical cavity. Since, the cavity-ring-down mirrors act as diverging lenses, a telescope was properly adjusted for divergence compensation.

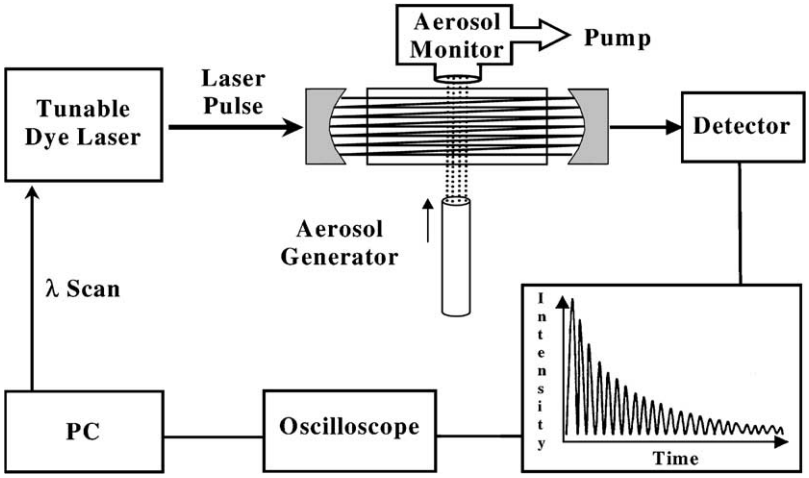

Fig. 1. Schematic diagramatic presentation of the CRLAS experimental set-up.

The ring-down signal was measured through the output mirror, using a metal package photomultiplier (Photosensor Module H6780-04, Hamamatsu, anode pulse rise time 0.8 ns). The signal was digitized and averaged over 128 laser pulses by a digital oscilloscope (LeCroy 9362, 1.5 GHz, 10 Gs s^{-1}) and then transferred to a personal computer for processing. The ring-down characteristic lifetime was determined for each averaged decay curve and the values obtained were averaged again over five consecutive measurement series. The observed ring-down characteristic lifetime in the above cavity, occupied with dry, filtered air, was about 1.7 μs. The air was dried and filtered by a silica-gel trap followed by a pyrex-glass filter (10–20 μm) and a syringe filter (0.2 μm).

2.2. Aerosols generation

NaCl and $CuCl_2 \cdot 2H_2O$ aerosols were generated at a wide range of sizes and concentrations by atomization of water solutions of the salts. Double ionized water was used for the solutions. The aerosol generator was based on a modified DeVilbiss (Model 40)-type nebulizer. The typical droplet size of this type of nebulizer was 3.0 μm-median mass diameter (MMD), with geometrical standard deviation (G.S.D.) of about 0.4 mm [41]. The aerosol concentration at the generator exit could be varied by modifying the overall airflow through atomizer and by controlling of the flow of the purging air. By varying the operating conditions and the concentrations of NaCl and $CuCl_2 \cdot 2H_2O$ solutions (10–200 g l^{-1}) we managed to obtain the required fraction of aerosol particles in the range of $d = 0.2$–2.0 μm. Aerosol diameter, d, can be expressed as a function to the size of initial liquid droplet [41].

$$d = d_D \left(\frac{C \rho_D}{\rho_p} \right)^{1/3} \quad (12)$$

where d_D is the droplet diameter, C the weight fraction of salt in the solution, ρ_D the droplet density and ρ_p is the aerosol particle density.

After atomizing, the flow of liquid aerosols was passed through a drying section comprised of a 80 cm glass tube (5 cm diameter), half packed with silica-gel. The out-coming aerosol particles were, thus water free, comprised solely of the examined compound.

In order to make sure that the salt aerosols were completely dry at the end of the drying section, we operated the generator with clean water and verified that no particles were detected by the aerosol monitor.

2.3. Aerosol introduction set-up

The optical cavity was surrounded by a Pyrex tube and continuously flashed by filtered, dry air. The aerosol flow from the atomizer was directed perpendicular to the cavity axis and introduced into the

Pyrex tube. Then, immediately after the cavity, it was pumped out through an aerosol monitor apparatus (process aerosol monitor PAM-510, Topas GmbH, Dresden, Germany) for concentration and size reference analysis. The effective diameter of the aerosol flow was 7 mm in the case of salt aerosols measurements. However, the indoor and outdoor aerosols were introduced such that the cavity was filled. All measurements were performed under atmospheric pressure.

2.4. Extinction efficiency calculation

The aerosol extinction efficiencies (Q_e), throughout this paper, were calculated using a Fortran program based on Bohren and Huffman algorithm for homogeneous spheres [36].

3. Results and discussion

3.1. Typical performance

We first attempted to evaluate the performance and the characteristic ring-down time of various aerosols at various concentrations. This step was carried out in order to examine the dynamic range of the ring-down times and its dependence upon particulate size and concentration. Typical results are as shown in Fig. 2, indicating that our CRLAS set-up is sensitive to aerosols of environmentally relevant size and concentration.

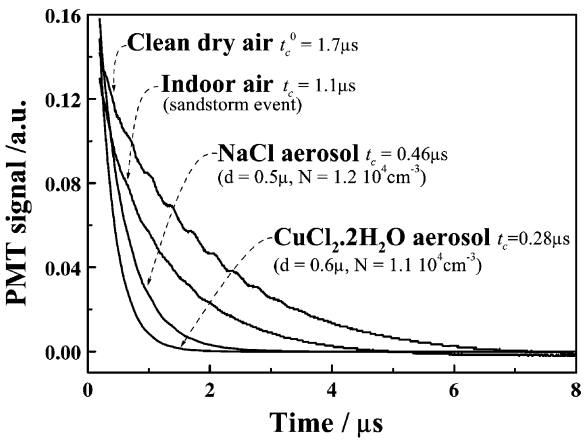

Fig. 2. Typical oscilloscope traces for clean air and various aerosols in the cavity. Note the sensitivity to particle size and concentration.

Four representative measurements are as shown in Fig. 2: (a) cavity with merely dry, filtered airflow (t_c^0); (b) indoor aerosols, measured on local sandstorm event; (c) NaCl aerosol flow, $d = 0.52\,\mu m$, $N = 1.2 \times 10^4\,cm^{-3}$; (d) $CuCl_2{\cdot}2H_2O$ aerosol flow, $d = 0.6\,\mu m$, $N = 1.1 \times 10^4\,cm^{-3}$ (d is the aerosol particulate diameter and N is the aerosol number concentration).

Several observations are noted:

(a) A significant decrease in cavity lifetime is obtained as aerosols are introduced into the ring-down cavity.
(b) The ring-down cavity set-up is sensitive enough for the detection of ambient indoor aerosols.
(c) Small variations in concentration and refractive index result in notable changes in ring-down cavity lifetimes.

3.2. Estimation of sensitivity

Let us now estimate the sensitivity of our CRLAS set-up, using the actual measurements and their standard deviation. The sensitivity is governed by the standard deviation of the aerosol extinction coefficient, σ_e, while t_c is directly measured. Therefore, it is necessary to calculate the propagation of error between these variables. Using Eq. (3), we obtain:

$$s_{\sigma_e} = \frac{nL}{cl}\sqrt{\frac{1}{t_c^4} + \frac{1}{(t_c^0)^4}}\, s_{t_c} \tag{13}$$

where s denotes absolute standard deviation. The actual absolute standard deviation of t_c measurements was about 5 ns. This deviation is equal to the time of one round trip of the probing pulse: $2L/c \cong 5$ ns. It corresponds to an relative standard deviation of about 0.25%, when $t_c = t_c^0 = 1.7\,\mu s$). At the above characteristic ring-down lifetime (1.7 μs), we find the absolute standard deviation of the calculated aerosol extinction coefficient as $8 \times 10^{-8}\,cm^{-1}$.

Clearly, the above figure could simply be improved, by straightforward experimental modifications. For example, one could apply a set of higher reflecting mirror, which are commercially available (but at a higher price). A characteristic lifetime of 50–100 μs and more could be easily achieved [32]. Note that t_c is at the

denominator of Eq. (13), thus, an improvement by a factor of more than two to three orders of magnitude is expected. However, experimental improvements can only approach an ultimate theoretical detection limit, as shown in the following.

It is interesting to estimate the ultimate performance of CRLAS in aerosol analysis. The theoretical sensitivity limit of aerosols detection is posed by Rayleigh scattering of atmospheric gases, which always causes a certain level of light extinction in the cavity. In this context, we should mention the CRLAS measurements by Naus and Ubachs [7], where the Rayleigh extinction of Ar, N_2 and SF_6 in the 560–650 nm region were measured. The Rayleigh scattering cross-section, ε_R, for our experimental conditions (wavelength of 620 nm and atmospheric pressure), is equal to 2.77×10^{-27} cm^2 [42]. Multiplying this value by the normal atmospheric concentration ($N = 2.69 \times 10^{19}$ cm^{-3}) gives the corresponding σ_e of 7.45×10^{-8} cm^{-1}. We can now use Eq. (3) for calculating the ring-down time caused by Rayleigh scattering. Assuming that the dominant cavity losses are due to Rayleigh scattering (large t_c^0, namely, perfect reflectivity of cavity mirrors), we obtain $t_c = 4.3 \times 10^{-4}$ s. This value can be used in Eq. (13) for calculating the ultimate standard deviation of the aerosol extinction coefficient. The actual standard deviation of t_c for this set-up is not precisely known, however, it can readily be estimated as one round trip time of the laser beam inside the cavity: $2L/c$ for our set-up is about 5 ns, which is the accuracy of the experimental electronic set-up. This way we obtain an estimation of the ultimate theoretical absorbance detection limit of about 1.4×10^{-12} cm^{-1}.

This is the minimum measurable extinction coefficient under ambient conditions, which can be considered as the theoretical sensitivity limit for pulse ring-down technique for aerosol detection in the atmosphere. Note that this calculation ignored beam absorption due to water and minor atmospheric gases, as well as scattering by air turbulences. The former problem could be solved using tuneable narrow band lasers, tuned far from overtone absorption bands. The latter problem is negligible at short resonators, compared to field measurements performed over hundreds of meters [43].

It should be mentioned that such performance is not yet achievable under current CRLAS techniques, however, experimental designs suitable for σ_e in the 10^{-12} cm^{-1} range, are already under planning [5]. At present, sensitivity depends on the reflectivity of cavity mirrors and is in the 10^{-10} cm^{-1} range [5,9,10].

3.3. Measurements of Q_e versus size parameter

An interesting aerosol characteristic, which is of theoretical and analytical importance, of the dependence of the aerosol extinction efficiency, Q_e, upon aerosol size parameter, α. Therefore, we experimentally examined this function using the CRLAS method. We tested various aerosol materials, characterized by different shapes and refraction indexes.

Characterization of the size parameter, α, requires independent information on the actual diameter of the examined aerosols. As previously described, independent information was obtained using process aerosol monitor (PAM 510). This device provides mean particle diameters and aerosol concentrations by measuring both the average transmission and the magnitude of fluctuations. The concentration number is calculated only from the magnitude of the transmission fluctuations, therefore, the results do not need any readjustments. However, the mean particle diameter provided by this method is a function of the aerosol refraction index and particulate geometrical shape. The instrumental readings are, therefore, based on the manufacturer calibration, which has been done for spherical aerosol particles characterized by refraction index of $n = 1.45$ (at 780 nm). Since our aerosols are of a different refractive index, we calculated a correction factor in order to obtain the real mean diameter values. It was calculated using the Bohren and Huffman program [36]. The corrections were obtained by comparison of particle extinction efficiency, Q_e, calculated for spherical aerosols of the actual refraction indexes. Here, all the particles were regarded as non-absorbing and of spherical shape.

Measurements of Q_e versus α were first performed for NaCl aerosols. The data is presented in Fig. 3. NaCl aerosols were generated as previously described. The atomizer was operated about 10 min before measuring, until flow stabilization was reached. First, t_c^0 value, i.e. the characteristic lifetime of the laser pulse in the optical cavity filled with dry air, was measured. The NaCl aerosol flow was then directed into the cavity, perpendicular to the optical axis and t_c was measured.

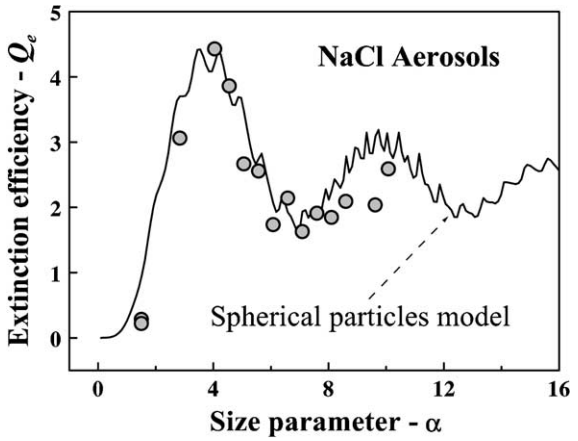

Fig. 3. Extinction efficiency of NaCl aerosols as a function of size parameter, α. The experimental results are compared to theoretical calculations for spherical particles of refraction index = 1.55 (solid curve).

Final results were obtained by averaging over more than 100 ring-down events for each point. The aerosol extinction coefficients, σ_e and the corresponding extinction efficiencies, Q_e, were calculated from Eqs. (3) and (8).

The thus obtained experimental Q_e values are presented in Fig. 3. The extinction efficiency initially increases with increasing the size parameter α and reaches a maximum value of about 4.5 at $\alpha = 4$. Q_e decreases below 2 at α of about 7, and then increases again. These experimental results are compared to the theoretical Q_e values, calculated for non-absorbing spherical aerosols of $n = 1.55$ [44]. It can be seen that there is a good correlation between the measurements and the calculations for $\alpha < 7$. In the region of the second peak there is some discrepancy between theory and measurements. This deviation could be attributed to the actual shape of real NaCl particulates, which is not spherical, as assumed in the theoretical calculations.

Measurements of extinction efficiency Q_e were performed for $CuCl_2{\cdot}2H_2O$ aerosols as well. This material was selected due to its higher refraction index and its different crystallite shape. $CuCl_2{\cdot}2H_2O$ has an orthorhombic crystal form—parallelepiped shape ($a : b : c = 0.9179{:}1{:}0.4627$) [45]. This way we can examine the performance of our measurement system over a wide range of these parameters.

Relevant to our theme is that the refraction index of these crystals depends on its orientation. Therefore, these crystals are characterized by three refraction index values: 1.644, 1.683 and 1.73 [45]. It means that Q_e versus α should depend on the particle orientation relative to the probing beam. However, since particulate orientations are randomized in our experimental set-up, one would expect results that are averaged over the three different values of Q_e.

Moreover, the actual shape of $CuCl_2{\cdot}2H_2O$ crystals does not allow for simplified model calculations assuming spherical particulates. Another complication that should be considered is the poly-dispersed character of $CuCl_2{\cdot}2H_2O$ aerosols.

The experimental results of Q_e versus α obtained for $CuCl_2{\cdot}2H_2O$ aerosols are presented in Fig. 4. The corresponding theoretical Q_e function, calculated for spherical aerosols (of $n = 1.68$) is also shown for comparison (solid curve). Although the general behavior of the experimental results is reproduced, a larger discrepancy is observed in this case, when the details are concerned. We also provide, for comparison, a different theoretical function, calculated for poly-dispersed aerosols (dashed curve) [36]. It seems that this curve fits somewhat better the experimental results, but still the discrepancy is not negligible. We tend to attribute the actual oscillating behavior of

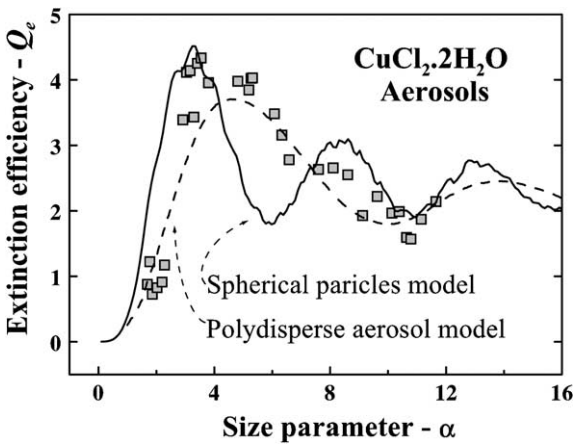

Fig. 4. Extinction efficiency of $CuCl_2{\cdot}2H_2O$ aerosols as a function of size parameter, α. The experimental results are compared to two theoretical calculations: for spherical particles of refraction index = 1.68 (solid curve) and for poly-dispersed spherical aerosols (dotted curve).

the experimental results to a combination of both the randomized crystal orientation and averaging over the poly-dispersed aerosols.

4. Conclusions

CRLAS has been applied to aerosol detection. The main conclusion derived from our results is that this method is suitable for sensitive detection of a variety of aerosols, under ambient conditions. It was found that small variations in concentration and in particulates' refractive index, result in notable changes in ring-down cavity lifetimes.

The actual sensitivity achieved by our preliminary set-up is as low as an extinction coefficient (σ_e) of $8 \times 10^{-8}\,cm^{-1}$. This performance can readily be improved using better optical components. The ultimate theoretical performance of CRLAS technique for aerosol detection was calculated: $\sigma_e = 1.4 \times 10^{-12}\,cm^{-1}$, which means detection capability of about 100 water particulates (of $d = 1\,mm$) per m^3. Taking into account the chemical speciation capability associated with this spectroscopic method, our findings indicate that CRLAS has the potential to become one of the most sensitive techniques for analysis of aerosols.

The experimental results presented in this study should be considered as one of the first attempt in this field and further investigation and experimental improvements are planned.

Acknowledgements

This research was supported by the Israel Science Foundation (Grant no. 112/1), by the James Franck Program in Laser Matter Interaction and by the Fund for promotion of research, Technion. Valery Bulatov is grateful for financial support by Ministry of Absorption for new immigrant scientists. Helpful discussions with S. Cheskis of Tel-Aviv University are much appreciated. Several discussions with A. Kachanov of Universitè Joseph Fourier, Grenoble and S. Panov of Massachusetts Institute of Technology are also acknowledged. We also thank V. Ryaboy of the Technion, Haifa, for assistance with the Fortran coding and calculations.

References

[1] A. O'Keefe, D.A.G. Deacon, Rev. Sci. Instrum. 59 (1988) 2544.
[2] J.J. Scherer, J.B. Paul, A. O'Keefe, R.J. Saykally, J. Chem. Rev. 97 (1997) 25.
[3] J.I. Steinfeld, Appl. Spectrosc. 54 (2000) 162A.
[4] M.D. Wheeler, S.T. Newman, A.J. Orr-Ewing, M.N.R. Ashfold, J. Chem. Soc., Faraday Trans. 94 (1998) 337.
[5] K.W. Busch, M.A. Busch (Eds.), Cavity-ring-down spectroscopy, an ultratrace absorption measurement technique, ACS Symp. Ser. (1999) 720.
[6] D. Romanini, P. Dupre, R. Jost, Vibrat. Spectrosc. 19 (1999) 93.
[7] H. Naus, W. Ubachs, Opt. Lett. 25 (2000) 347.
[8] G. Totsching, D.S. Baer, J. Wang, F. Winter, H. Hofbauer, R.K. Hanson, Appl. Opt. 39 (2000) 2009.
[9] A.A. Kachanov, D. Romanini, M. Chenevier, A. Garnache, F. Stoeckel, in: Proceedings of the SPIE-International Society of Optical Engineering on Air Monitoring and Detection of Chemical and Biological Agents II, vol. 3855, 1999, p. 51.
[10] J. Ye, J.L. Hall, Phys. Rev. Part A: Atom. Mol. Opt. Phys. 61 (2000) 061802/1.
[11] I. Labazan, S. Milosevic, AIP Conf. Proc. 559 (2001) 307.
[12] D. Kraus, R.J. Saykally, V.E. Bondybey, Chem. Phys. 247 (1999) 431.
[13] R.J. Saykally, Am. Chem. Soc. 221 (2001), Phys-047 (Abstract Paper).
[14] J.B. Paul, R.A. Provencal, C. Chapo, K. Roth, R. Casaes, R.J. Saykally, J. Phys. Chem. A 103 (1999) 2972.
[15] R.A. Provencal, J.B. Paul, K. Roth, C. Chapo, R. Casaes, R.J. Saykally, G.S. Tschumper, H.F. Schaefer, J. Chem. Phys. 110 (1999) 4258.
[16] R.A. Provencal, R. Casaes, K. Roth, J.B. Paul, C. Chapo, R.J. Saykally, G.S. Tschumper, H.F. Schaefer, J. Phys. Chem. 104 (2000) 1423.
[17] G.S. Tschumper, J.M. Gonzales, H.F. Schaefer, J. Chem. Phys. 111 (1999) 3027.
[18] A. O'Keefe, O. Lee, Am. Lab. 21 (1989) 19.
[19] S. Spuler, M. Linne, A. Sappey, S. Snyder, Appl. Opt. 39 (2000) 2480.
[20] M.D. King, E.M. Dick, W.R. Simpson, Atmos. Environ. 34 (2000) 685.
[21] H. Dahnke, D. Kleine, W. Urban, P. Hering, M. Murtz, Appl. Phys. B. 72 (2001) 121.
[22] J.J. Scherer, D.J. Rakestraw, Chem. Phys. Lett. 265 (1997) 169.
[23] I. Derzy, V.A. Lozovsky, S. Cheskis, Chem. Phys. Lett. 306 (1999) 319.
[24] I. Derzy, V.A. Lozovsky, N. Ditzian, I. Rahinov, S. Cheskis, Proc. Combust. Inst. 28 (2000) 1714.
[25] I. Derzy, V.A. Lozovsky, S. Cheskis, Israel J. Chem. 39 (1999) 49.
[26] S. Cheskis, I. Derzy, V.A. Lozovsky, A. Kachanov, D. Romanini, Appl. Phys. B. 66 (1998) 377.
[27] V.A. Lozovsky, I. Derzy, S. Cheskis, Chem. Phys. Lett. 284 (1998) 407.

[28] V.A. Lozovsky, I. Derzy, S. Cheskis, in: Proceedings of the 27th International Symposium on Combustion, 1998, p. 445.
[29] G. Meijer, M.G.H. Boogaarts, R.T. Jongma, D.H. Parker, A.M. Wodtke, Chem. Phys. Lett. 217 (1994) 112.
[30] J.J. Scherer, D. Voelkel, D.J. Rakestraw, Appl. Phys. B 64 (1997) 699.
[31] S.L. Logunov, Appl. Opt. 40 (2001) 1570.
[32] A.D. Sappey, E.S. Hill, T. Settersten, M.A. Linne, Opt. Lett. 23 (1998) 954.
[33] J.D. Smith, D.B. Atkinson, Analyst 126 (2001) 1216.
[34] R.L. Vander Wal, T.M. Ticich, Appl. Opt. 38 (1999) 1444.
[35] W.C. Hinds, Properties, behaviour and measurements of airborne particles, in: Aerosol Technology, Wiley, New York, 1982, p. 315.
[36] C.F. Bohren, D.R. Huffman, Absorption and Scattering of Light by Small Particles, Wiley, New York, 1998, p. 287.
[37] W.E. Wilson, P.C. Reist, Atmos. Environ. 28 (1984) 803.
[38] J.V. Dave, Sub-Routines for Computing the Parameters of the Electromagnetic Radiation Scattered by a Sphere, IBM Order number 360D-17.4.002, 1968.
[39] W.J. Wiscombe, Mie scattering calculations, NCAR/TN-140+ STR, National Center for Atmospheric Research, Boulder Co., 1979.
[40] W.J. Wiscombe, Appl. Opt. 19 (1980) 1505.
[41] N. Corn, N.A. Esmen, in: R. Dennis (Ed.), Handbook on Aerosols, National Technical Information Service, US Department of Commerce, Springfield, 1976, p. 9.
[42] A. Bucholtz, Appl. Opt. 34 (1995) 2765.
[43] W.C. Malm, J.V. Molenar, R.A. Eldred, J.F. Sisler, J. Geophys. Res. D 101 (1996) 19251.
[44] Handbook of Chemistry and Physics, 67th Edition, CRC Press, Boca Raton, FL, USA.
[45] J.D.H. Donnay (Ed.), Crystal Data Determination Tables, ASA Monograph NS, American Crystallographic Association, 1963.